Available online at http://www.journalcra.com

International Journal of Current Research
Vol. 7, Issue, 08, pp.19542-19547, August, 2015

INTERNATIONAL JOURNAL OF CURRENT RESEARCH

ISSN: 0975-833X

RESEARCH ARTICLE

APPLICATION OF EULERIAN AND LAGRANGIAN COUPLINGS TO ESTIMATE THE INFLUENCE OF SHOCK PRESSURE LOADING ON THE SUBMERSIBLE HULL USING FINITE ELEMENT ANALYSIS

*Chennakesava Reddy, A.

Department of Mechanical Engineering, JNTUH College of Engineering, Kukatpally, Hyderabad, Telangana State, India

ARTICLE INFO

Article History:
Received 27th May, 2015
Received in revised form
15th June, 2015
Accepted 26th July, 2015
Published online 31st August, 2015

Key words:
Submersible hull,
Shock pressure load,
Finite element analysis,
Eulerian-Lagrangian coupling.

ABSTRACT

The aim was to estimate the influence of shock pressure loading on the submersible hull using finite element analysis. The fluid medium was molded based on Tait's equation of state. The equation of state from Jones-Wilkins-Lee (JWL) was used to describe the detonation products of explosives. The explosion and fluid were interfaced using Eulerian-Eulerian coupling and the fluid and shell were interfaced using arbitrary Lagrangian-Eulerian coupling. The damage has occurred in the submersible hull surface exposed to explosion only.

Citation: Chennakesava Reddy, A., 2015. "Application of Eulerian and Lagrangian couplings to estimate the influence of shock pressure loading on the submersible hull using finite element analysis", *International Journal of Current Research*, 7, (8), 19542-19547.

INTRODUCTION

Underwater explosions are very important and complex problems for naval surface ships or submarines, since detonations near a ship can damage the vessel. The inelastic behavior of structures to dynamic loads such as impulse, blast and underwater shock is of great importance in many fields such as marine and ocean industries. The problem is fairly complex involving material and geometric non-liniearities. Huang and Kiddy (1995) studied the transient interaction of a spherical shell with an underwater explosion shock wave and subsequent pulsating bubble, based on their approach on the finite element method coupled with the Eulerian–Lagrangian method. According to their results, the structural response, as well as interactions among the initial shock wave, the structure, its surrounding media and the explosion bubble must be considered. Kwon and Fox (1993) applied numerical and experimental techniques to investigate the nonlinear dynamic response of a cylinder subjected to a side-on, far-field underwater explosion. Comparisons between the strain gage measurements and the numerical results at different locations revealed a good agreement. Shin and Chisum (1997) employed a coupled Lagrangian–Eulerian finite element analysis technique as a basis to investigate the response of an infinite cylindrical and a spherical shell subjected to a plane acoustic step wave. When a submerged structure subjected to underwater explosion loading, it is important to predict the structural response to the shock wave. Furthermore, in the case of the explosion occurring close to the structure, a high velocity water jet penetrating the gas bubble occurs. This water jet is extremely efficient in producing damage. The purpose of this paper was to demonstrate the application of Eulerian-Eulerian coupling to interface the explosion and fluid medium and Lagrangian-Eulerian coupling to interface the fluid and submersible hull. The objective was also to estimate the influence of shock pressure loading on the submersible hull using finite element analysis.

Theoretical background

The sequence of underwater explosion and finite element modeling are discussed.

Shock wave pressure: The underwater shock wave generated by the explosion is superimposed on the hydrostatic pressure.

Corresponding author: Chennakesava Reddy, A.
Department of Mechanical Engineering, JNTUH College of Engineering, Kukatpally, Hyderabad, Telangana State, India.

The pressure history $P(t)$ of the shock wave at a fixed location starts with an instantaneous pressure increase to a peak P_{max} followed by a decline which initially is usually approximated by an exponential function. Thus, according to the empirical equation of Cole (1948):

$$P(t) = P_o e^{-t/\theta} \quad 0 \ll t \ll \theta \qquad (1)$$

The peak pressure (P_o) and the decay constant (θ) are given by

$$P_o = 52.16 \times 10^6 \left(W^{1/3}/R\right)^{1.13} \qquad (2)$$

$$\theta = 92.5 \times W^{1/3}\left(W^{1/3}/R\right)^{-0.22} \qquad (3)$$

where W is the charge weight (kg) and R is the stand-off distance (m).

Because of the spherical spreading nature of the shock wave, the wave reaches different locations at different times, i.e. there is time delay. The time delay (t_d) can be calculated using the radial distance at any location (R), the shortest radial distance (R_o) and the sound wave velocity (c), as follows:

$$t_d = (R - R_o)/c \qquad (4)$$

By incorporating the time delay, Eq. (1) is rewritten in the following form:

$$P(t) = P_o e^{-(t-t_d)/\theta} \quad 0 \ll t \ll \theta \qquad (5)$$

Shock wave velocity

As the wave travels from the explosion, the profile of the shock wave broadens and the amplitude reduces as shown in Fig.1.

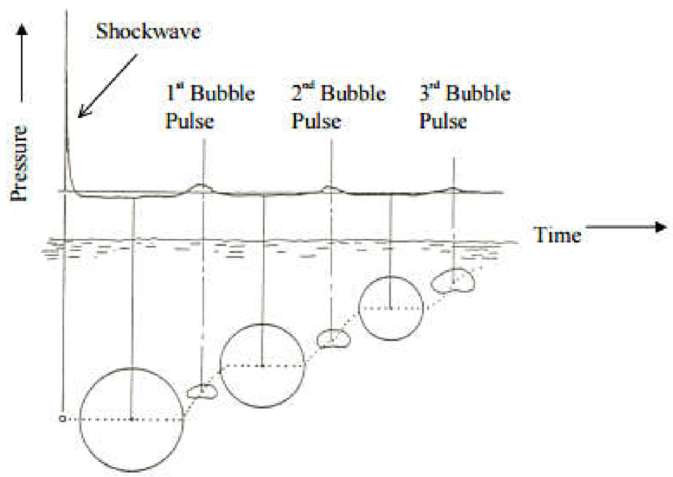

Fig.1. Pressure waves and bubble phenomena of underwater explosion

The velocity in the vicinity of the explosion depends on the peak pressure of the shock wave and the acoustic velocity, as given by

$$c_s = c_a \times (1 + 6 \times 10^{-10} P_o) \qquad (6)$$

As the shock wave propagates, it sets the water particle in the vicinity in motion. The water particle velocity associated with the shock wave is given by

$$v(t) = P(t)/\rho c \qquad (7)$$

where ρ is the density of the fluid medium.

The initial high pressure in the product gases of explosion decreases considerably after the primary shock pulse is emitted. The inside pressure in the gas bubble is much higher than the surrounding hydrostatic pressure, which tends to push the water and expand the gas bubble. At this stage, the gas bubble expands rapidly and consequently the pressure inside the bubble decreases and the kinetic energy accelerates the surrounding water till the bubble expands to the maximum. As the gas bubble expands to the maximum radius, the gas pressure falls below the hydrostatic pressure, the contraction of gas bubble starts and continues until the pressure inside becomes insignificant. Hence, the gas bubble undergoes repeated cycles of expansion and contraction. The maximum radius (R_{max}) during the first pulsation and the duration (T) of the first pulsation are given by

$$R_{max} = 3.3 \times (W/Z_o)^{1/3} \qquad (8)$$

$$T = 2.06 \times \left(W^{1/3}/{Z_o}^{5/6}\right) \qquad (9)$$

$$Z_o = D + 10 \qquad (10)$$

where, D is water depth, Z_o is the reference depth.

Secondary shock wave

During the contraction phase of the gas bubble oscillation, when the bubble reaches its minimum, a pressure pulse known as the secondary shock wave, of small amplitude is emitted. The peak pressure of the secondary pressure pulse is given by

$$P_2 = 2590 \times \left(W^{1/3}/R\right) \qquad (11)$$

Gas bubble migration

When the gas bubble has last buoyancy, the migration of gas bubble occurs. The migration of the gas bubble from the location of the explosive charge up to the location corresponding to the first bubble pulse is given by

$$m = (90/Z_o)W^{1/2} \qquad (12)$$

Hull shock factor

Since a ship can be subjected to a large variety of underwater explosion (variation in charge weight, standoff distance), the relation between attack severity and geometry must be determined (Fig.2). For damage predictions for submarines, this factor is referred to as the Hull Shock Factor (HSF). It has been found that

$$\mathrm{HSF} = \sqrt{W}/R \qquad (13)$$

Where, W is the charge weight and R is the standoff distance.

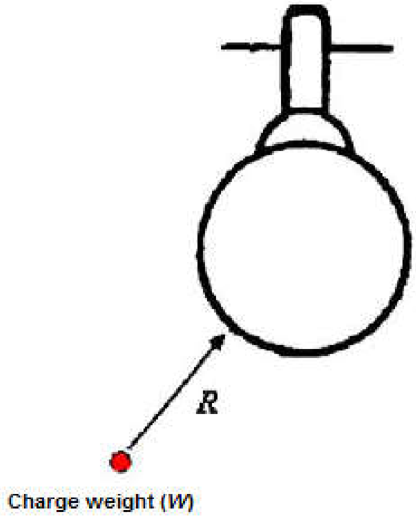

Fig.2. Hull shock factor

Finite element modeling

For a fully or partially submerged structure subjected to an underwater shock wave, the structure may exhibit material and geometrical nonlinear behavior. Based on the theorem of virtual displacement, the governing equation of the problem can be expressed in matrix form (Chennakesava R Alavala, 2008) as given below:

$$[M_s]\{\ddot{u}\} + [C_s]\{\dot{u}\} + [K_s]\{u\} = \{f\} \tag{14}$$

where,

$[M_s] = \int \rho_s [N]^T [N] dv$, $[C_s] = \int \rho_s \alpha_c [N]^T [N] dv$, $[K_s] = \int [B]^T [D][B] dv$ and $\{f\} = \int [N]^T f dv$

$[M_s]$, $[C_s]$ and $[K_s]$ are the structural mass, damping and stiffness matrices, respectively. $[N]$, $[B]$ and $[D]$ are the shape function, strain matrix and matrix of elastic-plastic tangent stiffness, respectively. $\{u\}$ and $\{f\}$ are the structural displacement and the external force vector, respectively. For a structure submerged in an infinite acoustic medium, the governing equation of the wet surface of the shell is based on the Doubly Asymptotic Approximation as given below:

$$[M_f]\{\ddot{P}_s\} + \rho_f c[A_f]\{\dot{P}_s\} + \rho_f c[\varphi_f][A_f]\{P_f\} = \rho_f c[M_f]\{\dot{v}_s\} + [\varphi_f][M_f]\{v_s\} \tag{15}$$

Where

$$[\varphi_f] = \alpha \rho_f c[A_f][M_f]^{-1} \tag{16}$$

$[M_f]$ is the symmetric fluid mass matrix α is the scale parameter bounded $0 \ll \alpha \ll 1$, ρ_f and c are the fluid density and sound velocity, respectively. $\{v_s\}$ is the vector of scattered-wave fluid particle velocities normal to the structural surface. The fluid surface is coupled to the structural response by the following equation

$$\{v_s\} = [G]^T\{\dot{u}\} - \{v_i\} \tag{17}$$

where $\{v_i\}$ is the fluid incident velocity.

MATERIALS AND METHODS

The physical model of a submersible hull is shown Fig.3.

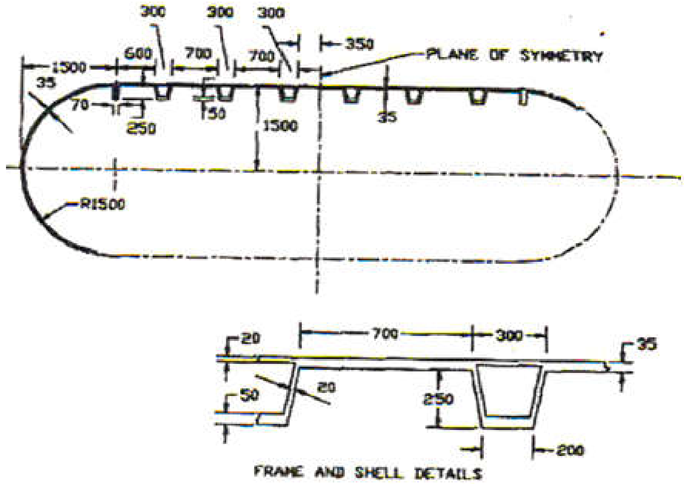

Fig. 3. Physical model of submersible hull

The major dimensions of the submersible hull are as follows:

Diameter = 3 m
Length= 9.5 m
Thickness = 0.035 m

The finite element analysis of the submersible hull was carried out using DYTRAN non-linear finite element code. For the finite element analysis, the explosion, fluid and submersible hull were modeled as an integral unit. The fluid and explosion were meshed with 8 node Eulerian solid element (figure 4a). The number of elements was 106160. The fluid domain of 5 m width in transverse direction and 3 m width in the longitudinal direction from the submersible hull was considered for modeling. The submersible hull was discretized with 4 node Lagrangian element (figure 4b).

The number of elements was 7708. The explosion and fluid were interfaced using an Eulerian-Eulerian coupling. The fluid and the submersible hull were interfaced using Lagrangian-Eulerian coupling. In the present investigation, the explosion was assumed on the normal line passing through the centerline of the submersible hull at a distance of 5 m.

The exploded charge weight was varied from 1kg to 25 kg. For the finite element analysis, the fluid was modeled using Eulerian solid element with Tait's equation of state and the explosion was modeled using Eulerian solid element with JWL equation of state. The material constants used in the Tait's equation of state are as follows:

$\rho = 1025\ kg/m^3$
$a = 48402.7105\ Pa$
$b = 3.01E8$ Pa
$R = 7.15$
$C_0 = 1450\ m/s$

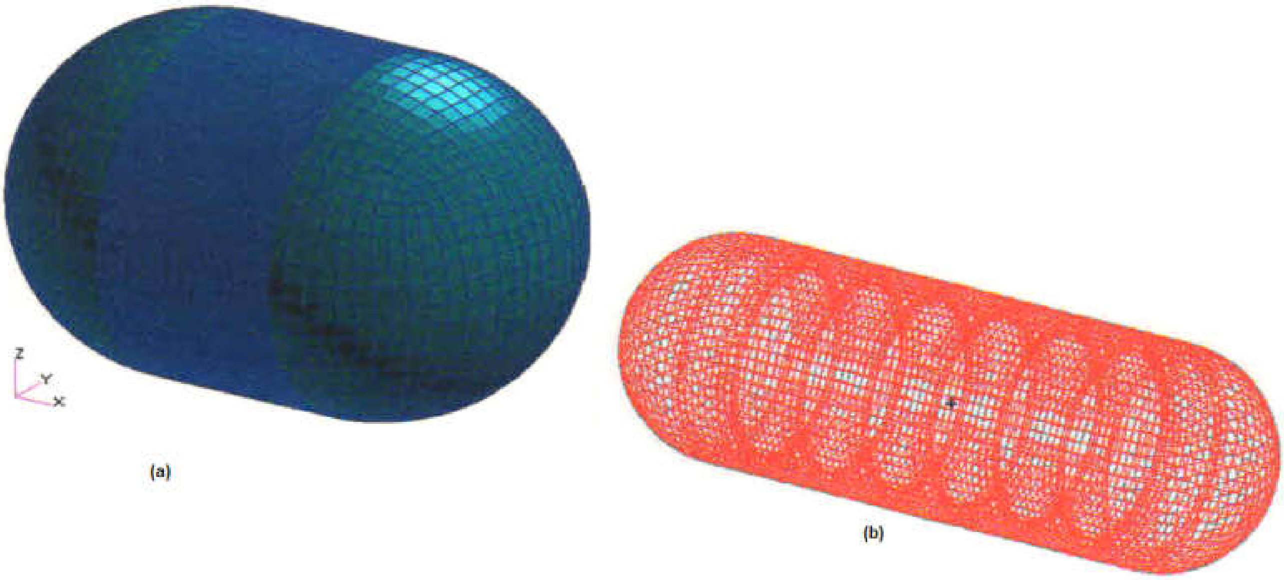

Fig. 4. Finite element modeling (a) fluid domain and explosion and (b) submersible hull

The equation of state from Jones-Wilkins-Lee (JWL) is used to describe the detonation products of explosives.

$$p = A\left(1 - \frac{\omega}{R_1 V}\right)\exp(-R_1.V) + B\left(1 - \frac{\omega}{R_2 V}\right)\exp(-R_{12}.V) + \frac{\omega e_0}{V} \quad (18)$$

The ratio $V = \rho_e/\rho$ is defined by using ρ_e is the density of explosive (solid part) and ρ is the density of detonation products. The parameters *A, B,* R_1, R_2 and ω are given below:

$\rho = 1610\ kg/m^3$
$A = 371.2\ GPa$
$B = 3.2306\ GPa$
$R_1 = 4.15$
$R_2 = 0.95$
$\omega = 0.3$

The submersible hull was made of elasto-plastic mild steel with isotropic hardening. Cowper-Symonds relation is used to model the strain rate effects. The material properties are given below:

$E = 210\ GPa$
$v = 0.3$
$G_{12} = 9.955\ GPa$
$\sigma_x = \sigma_y = 250\ MPa$
$\rho = 7860\ kg/m^3$

Constants of Copwper-Symonds relation are D = 40 and n = 5. Dynamic effects of strain rates are taken into account by scaling static yield stress with the factor, assumed by Cowper –Symonds relation:

$$\sigma_d/\sigma_s = 1 + (\dot{\varepsilon}/D)^{1/n} \quad (19)$$

where, σ_d is the dynamic stress; σ_s is the static stress; $\dot{\varepsilon}$ is the strain rate; and D and n are constants of Cowper –Symonds relation.

The analysis of the coupled field problem was solved using explicit integration scheme. Three incremental time steps of 0.05, 0.1 and 0.2 microseconds were used for the analysis. The explosion and fluid were interfaced using Eulerian-Eulerian coupling and the fluid and shell were interfaced using arbitrary Lagrangian-Eulerian coupling. The initial conditions used in the explosion were specific internal energy (4.16 x 10^6 K/kg) and detonation velocity (6730 m/s). The explosive element was modeled using eight node Eulerian solid elements. The element length was 0.426 m. The stand-off distance was 5 m.

RESULTS AND DISCUSSION

The shock pressure loading of the fluid medium was applied on the surface of on the submersible hull through arbitrary Lagrangian-Eulerian coupling. The peak pressures were calculated for all the cases are given in Table 1. The peak value was 36 MPa for a charge weight of 25 kg.

Table 1. Peak shock pressure loads

Charge weight (W), kg	Shock factor, $\sqrt{kg/m}$	Shock pressure, MPa
1	0.09	9
2	0.12	13
5	0.20	18
10	0.28	22
15	0.34	25
20	0.40	30
25	0.45	36

Displacement-Time History

The displacement-time history of the submersible hull exposed to the explosion for a charge weight of 25 kg is shown in Fig.5. The deformation of the submerged hull was obtained from the maximum displacement by subtracting the elastic deformation. The maximum displacement was 0.00509 m at 7.602 milliseconds. The maximum plastic displacement of the submerged hull was 0.0459 m. The displacement contours are shown in Fig.6. The plastic displacement was found to be high on the submersible hull side exposed to the explosion (Fig.6a). The elastic displacement was found on the rear side of submersible hull away from the explosion (Fig.6b). There was no plastic displacement on the rear side of submersible hull.

Strain-Time History

The effective plastic strain of the submersible hull subjected to for the explosion charge weight of 25 kg is shown in Fig.7. The plastic stain was increased until about 4 milliseconds and then became constant.

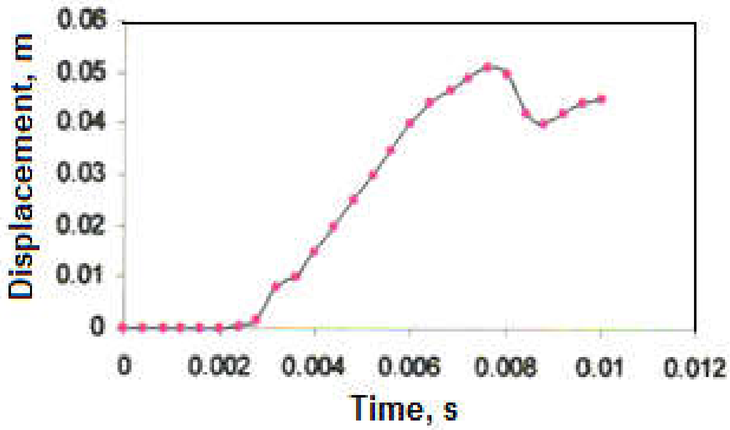

Fig. 5. Displacement-time history for charge weight of 25 kg

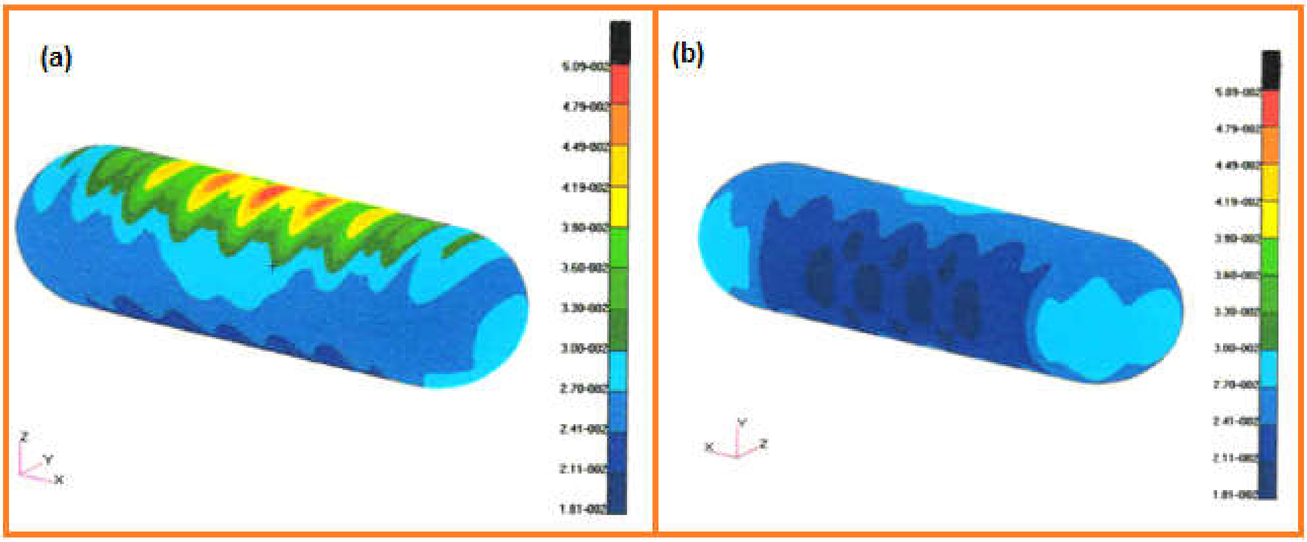

Fig. 6. Displacement of submerged hull at HSF = 0.45 (a) surface exposed to explosion and (b) Surface on the rear side of submersible hull

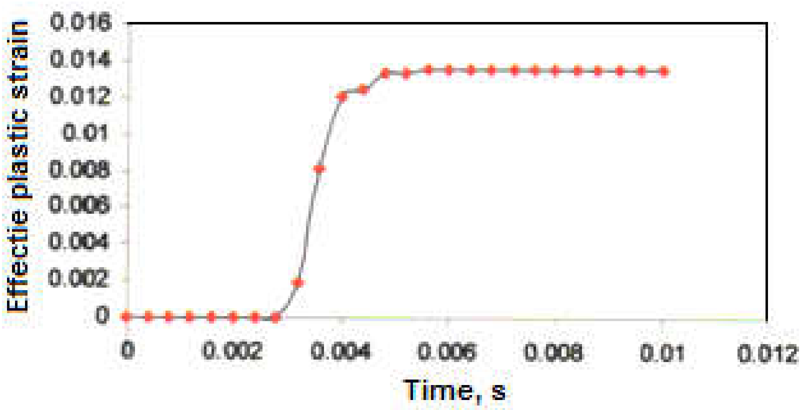

Fig. 7. Strain-time history for charge weight of 25 kg

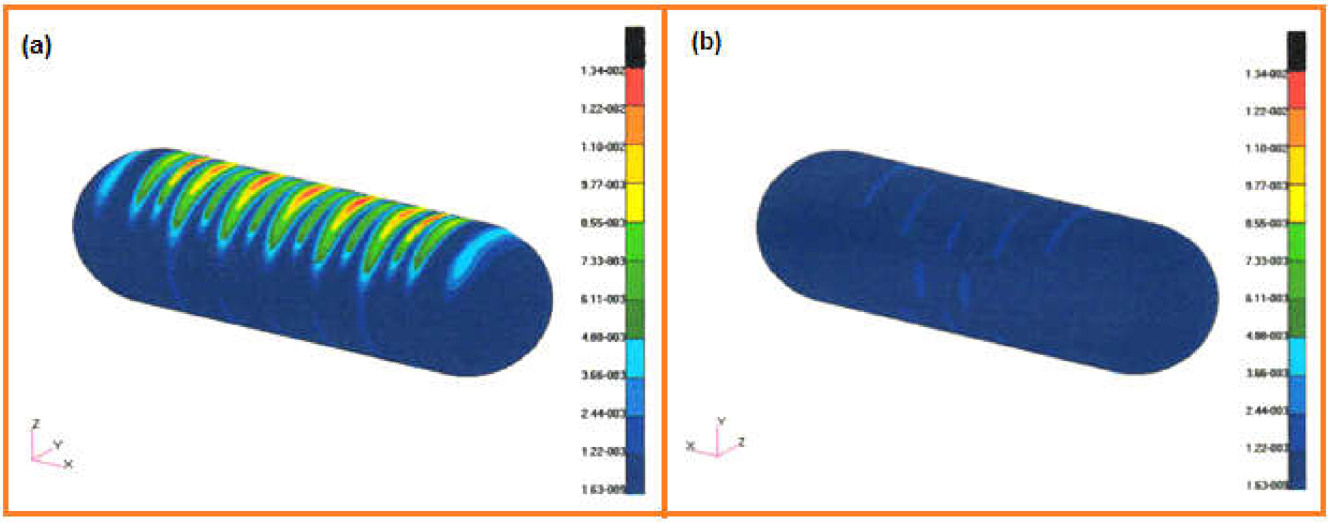

Fig. 8. Effective plastic strain of submerged hull at SF = 0.45 (a) surface exposed to explosion and (b) surface on the rear side of submersible hull

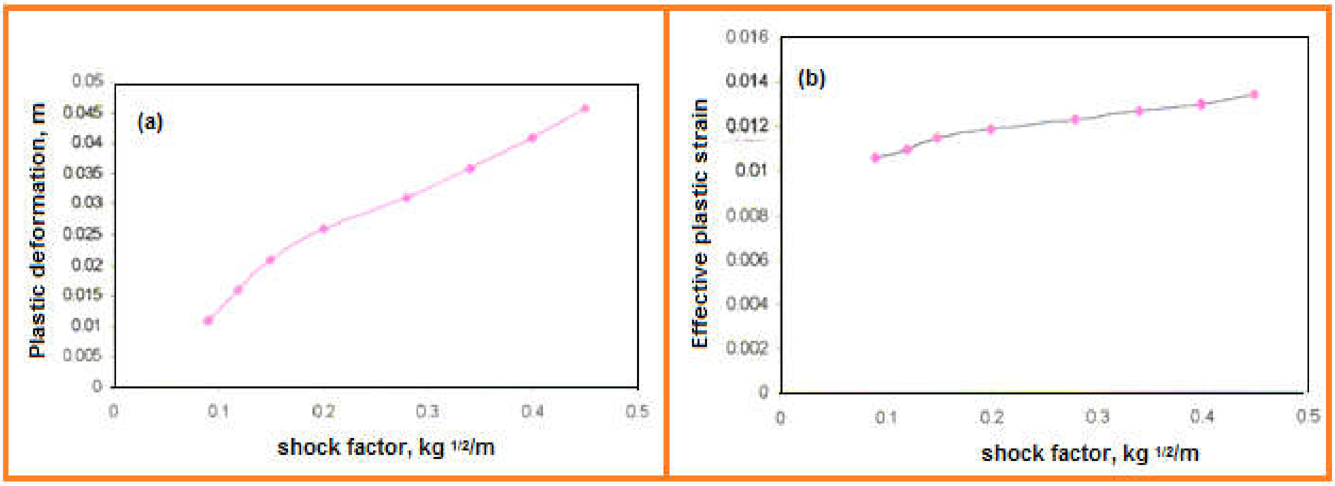

Fig. 9. Impact of shock load deflection (a) deformation (b) plastic strain

The plastic strain was found to be high on the submersible hull side exposed to the explosion (Figure 8a). The elastic strain was found on the rear side of submersible hull away from the explosion (Figure 8b). There was elastic strain on the rear side of submersible hull.

Impact of Shock Wave

The deformation increases with the increase of shock load as shown in Fig.9a. The same kind of trend is observed with the plastic strain (Fig.9b). The effective plastic strain was much less than the rupture strain of the mild steel. Hence, tearing or rupture in the submersible hull was not detected.

Conclusion

The plastic displacement of the submerged hull has been found to be 0.0459 m for explosion charge of 25 kg. The damage has occurred in the submersible hull surface exposed to explosion only.

REFERENCES

Chennakesava R. Alavala, 2008. Finite Element Methods: Basic Concepts and Applications, PHI Learning Pvt. Ltd., New Delhi.

Cole, R.H. 1948. Underwater Explosions. Princeton University Press, Princeton.

Huang, H., Kiddy, K.C. 1995. Transient interaction of a spherical shell with an underwater explosion shock wave and subsequent pulsating bubble. Shock and Vibration, 2:451–460.

Kwon, Y.W. and Fox, P.K. 1993. Underwater shock response of a cylinder subjected to a side-on explosion. Comp. & Struct., 48(4): 637–646.

Shin, Y.S. and Chisum, J.E. 1997. Modeling and simulation of underwater shock problems using a coupled lagrangian-eulerian analysis approach. Shock and Vibration, 4:1–10.

****